

Different T Cell Receptor Affinity Thresholds and CD8 Coreceptor Dependence Govern Cytotoxic T Lymphocyte Activation and Tetramer Binding Properties*

Received for publication, February 1, 2007, and in revised form, April 23, 2007. Published, JBC Papers in Press, May 31, 2007, DOI 10.1074/jbc.M700976200

Bruno Laugel^{†1}, Hugo A. van den Berg[§], Emma Gostick[‡], David K. Cole[¶], Linda Wooldridge[¶], Jonathan Boulter[¶], Anita Milicic[‡], David A. Price[‡], and Andrew K. Sewell^{†1,2}

From the [†]Nuffield Department of Medicine, John Radcliffe Hospital, University of Oxford, Oxford OX3 9DU, United Kingdom, the [§]Warwick Systems Biology Centre, University of Warwick, Coventry CU4 7AC, United Kingdom, and the [¶]Department of Medical Biochemistry and Immunology, Cardiff University School of Medicine, Cardiff CF14 4XN, Wales, United Kingdom

T cells have evolved a unique system of ligand recognition involving an antigen T cell receptor (TCR) and a coreceptor that integrate stimuli provided by the engagement of peptide-major histocompatibility complex (pMHC) antigens. Here, we use altered pMHC class I (pMHCI) molecules with impaired CD8 binding (CD8-null) to quantify the contribution of coreceptor extracellular binding to (i) the engagement of soluble tetrameric pMHCI molecules, (ii) the kinetics of TCR/pMHCI interactions on live cytotoxic T lymphocytes (CTLs), and (iii) the activation of CTLs by cell-surface antigenic determinants. Our data indicate that the CD8 coreceptor substantially enhances binding efficiency at suboptimal TCR/pMHCI affinities through effects on both association and dissociation rates. Interestingly, coreceptor requirements for efficient tetramer labeling of CTLs or for CTL activation by determinants displayed on the cell surface operated in different TCR/pMHCI affinity ranges. Wild-type and CD8-null pMHCI tetramers required monomeric affinities for cognate TCRs of $K_D < \sim 80 \mu\text{M}$ and $\sim 35 \mu\text{M}$, respectively, to label human CTLs at 37 °C. In contrast, activation by cellular pMHCI molecules was strictly dependent on CD8 binding only for TCR/pMHCI interactions with K_D values $> 200 \mu\text{M}$. Altogether, our data provide information on the binding interplay between CD8 and the TCR and support a model of CTL activation in which the extent of coreceptor dependence is inversely correlated to TCR/pMHCI affinity. In addition, the results reported here define the range of TCR/pMHCI affinities required for the detection of antigen-specific CTLs by flow cytometry.

In concert with the T cell receptor (TCR),³ the coreceptors CD4 and CD8 participate in and enhance the process of antigen

recognition by T cells through extracellular interactions with peptide-major histocompatibility complex (pMHC) molecules (1–3) and amplification of ensuing signal transduction events (4–8). CD8 molecules are predominantly expressed as $\alpha\beta$ heterodimers on the surface of cytotoxic T lymphocytes (CTLs) (9), but are also found in $\alpha\alpha$ homodimeric form on intraepithelial $\alpha\beta$ T lymphocytes, certain subsets of circulating activated CTLs, and the membranes of distinct cell lineages such as $\gamma\delta$ T cells, natural killer T cells, and dendritic cells (reviewed in Ref. 10). CD8 $\alpha\alpha$ and CD8 $\alpha\beta$ bind directly to invariant domains of major histocompatibility complex class I (MHCI) molecules (11–13). Although CD8 $\alpha\alpha$ and CD8 $\alpha\beta$ bind MHCI molecules with similar affinities (14), it is well established that CD8 $\alpha\alpha$ is a much poorer coreceptor for CTLs than is CD8 $\alpha\beta$. Indeed, an emerging concept is that CD8 $\alpha\alpha$ acts as an inhibitor of CTL activation (10). More generally, recent experimental evidence has lent credence to the hypothesis that efficient regulation of CTL activity is mediated by modifications of CD8 coreceptor functions *in vivo*. These modifications include switching to expression of the CD8 $\alpha\alpha$ homodimer, post-translational changes of CD8 $\alpha\beta$ following activation (15, 16), and down-regulation of CD8 expression on the cell surface (17–20). Fluctuations in the partitioning and relative distribution of TCR and CD8 molecules on the membrane have also been proposed to influence the interplay between the antigen receptor and coreceptor in the initiating steps of CTL activation. Notably, Pecht and Gakamsky (21) proposed a model in which pre-existing TCR-CD8 complexes constitutively formed on the surface of non-activated CTLs are crucial for the initiation of CTL activation. This hypothesis stems from observations that blocking CD8 engagement and disrupting T cell membrane microdomain organization substantially decrease the binding efficiency and association kinetics of multimeric peptide-major histocompatibility complex class I (pMHCI) molecules (22). This model, together with studies reporting that variations in the glycosylation state and expression levels of CD8 following *in vivo* antigen encounter affect the binding of pMHCI multimers to CTLs (19, 20), suggests that inhibition of the extracellular engagement of pMHCI by CD8 results in reduced CTL activa-

complex class I; hTERT, human telomerase reverse transcriptase; HLA, human leukocyte antigen; IFN- γ , interferon- γ ; HIV-1, human immunodeficiency virus-1; WT, wild-type; MFI, mean fluorescence intensity; SPR, surface plasmon resonance.

* The costs of publication of this article were defrayed in part by the payment of page charges. This article must therefore be hereby marked "advertisement" in accordance with 18 U.S.C. Section 1734 solely to indicate this fact.

¹ Present address: Ludwig Inst. for Cancer Research, Chemin des Boveresses 155, 1066 Epalinges, Switzerland.

² To whom correspondence should be addressed: Dept. of Medical Biochemistry and Immunology, Cardiff University School of Medicine, Henry Wellcome Bldg., Heath Park, South Parks Rd., Cardiff CF14 4XN, Wales, United Kingdom. Tel.: 44-2920-744-003; Fax: 44-2920-745-111; E-mail: sewellak@cardiff.ac.uk.

³ The abbreviations used are: TCR, T cell receptor; pMHC, peptide-major histocompatibility complex; CTLs, cytotoxic T lymphocytes; MHCI, major histocompatibility complex class I; pMHCI, peptide-major histocompatibility

Coreceptor Dependence of CTL Activation and Tetramer Binding

tion and can therefore act as a mechanism to regulate the process of antigen recognition independently from coreceptor signaling properties.

The recognition efficiency of all syngeneic pMHC I epitopes is improved by CD8 coreceptor activities. However, the absence of the coreceptor from the cell surface or abrogation of its engagement with MHC molecules does not inhibit T cell activation by different agonist ligands to the same extent (23–26). Activation of a T cell by different epitope variants is thus said to differ in its degree of coreceptor dependence. Two principal, mutually nonexclusive explanations for this phenomenon have been proposed in the CD8 system. First, data obtained by Holler and Kranz (27) and others (23, 25, 28) strongly suggest that coreceptor dependence is inversely correlated with TCR/pMHC I affinity. In this model, CTL activation by weak agonist ligands characterized by low affinity and short half-life interactions with the TCR relies heavily on CD8 coreceptor activity. Second, it has been proposed that positioning of the TCR variable domains ($V\alpha$ in particular) on the pMHC I platform and the resulting overall conformation of the TCR $\alpha\beta$ -CD3 complex may hamper the signaling activity of CD8 (29) and compromise its ability to engage MHC I molecules through binding solutions offering unfavorable positioning of the TCR/pMHC I/CD8 trimolecular complex (30). Therefore, in this model, coreceptor enhancement of CTL activation depends on the geometry of TCR engagement.

In this study, we describe a system that enabled us to examine the effects of the pMHC I/CD8 interaction on the engagement of antigenic ligands by CTLs as a function of TCR/pMHC I affinity. Comparison of the influence of CD8 on the binding efficiency of various soluble pMHC I complexes and on the corresponding cellular activation profiles elicited by these ligands presented on the surface of antigen-presenting cells provides insights into the role of the coreceptor extracellular binding properties in CTL activation.

EXPERIMENTAL PROCEDURES

Cell Lines—The CTL clone ILA1, isolated from a healthy donor, is specific for residues 540–548 (ILAKFLHWL) of the catalytic subunit of the ubiquitous tumor-associated antigen human telomerase reverse transcriptase (hTERT) presented in association with human leukocyte antigen (HLA) A*0201 (HLA A2 from hereon). Peripheral blood mononuclear cells were stimulated by autologous antigenic presentation using the hTERT-(540–548) peptide at 10 μ M in the presence of interleukin-7. Three days after initial antigen exposure, interleukin-2 was gradually added to the culture up to 100 units/ml. Similar rounds of re-stimulation were repeated three times every 12–14 days. Following successful expansion, an antigen-specific T cell line was sorted on the basis of the expression of the activation markers CD25 and CD69 after incubation with the ILAKFLHWL peptide using a FACSVantage (BD Biosciences). The monoclonal T cell line ILA1 was produced by limiting dilution of this enriched line. T cells were initially grown in RPMI 1640 medium (Sigma) supplemented with 10% fetal calf serum, 2 mM L-glutamine, 100 units/ml penicillin, and 100 μ g/ml streptomycin (R10) with 10% T-STIM (final volume; BD Biosciences) and 100 units/ml interleukin-2 and containing

mixed irradiated allogeneic feeders from three unrelated donors. The general methods employed for the generation and maintenance of the other CTL lines used in this study were described previously (31). Hmy2.C1R transfectant cells expressing HLA A2 were used in all functional assays (32). These cells were maintained in R10.

Interferon- γ (IFN- γ) ELISpot—Antigen-presenting cells (50,000/well; Hmy2.C1R transfectants) in 100 μ l of R10 were added to ELISpot plates (Millipore Corp.) coated with anti-human IFN- γ monoclonal antibody (Mabtech AB). CTLs were then added in 100 μ l of R10. Peptides were mixed with the cells at the indicated final concentrations. After incubation at 37 $^{\circ}$ C for 4 h, the plates were washed six times with phosphate-buffered saline, and a secondary biotinylated anti-human IFN- γ monoclonal antibody (D1K, Mabtech) was added for 90 min. The plates were then washed again, incubated with alkaline phosphatase-conjugated streptavidin, and developed with a colorimetric reagent according to the manufacturer's instructions. Spots were counted using an automated ELISpot reader (Autoimmun Diagnostika GmbH).

Degranulation Assays—These assays were carried out as described previously (33). 10,000 CTLs were mixed with 50,000 antigen-presenting cells in the presence of the indicated final peptide concentrations.

Measurement of TCR Down-regulation—10,000 antigen-presenting cells were prepulsed with the indicated concentrations of peptide and washed twice with serum-free RPMI 1640 medium supplemented with penicillin, streptomycin, and L-glutamine as above. 30,000 CTLs were added in each assay well and incubated for 4 h at 37 $^{\circ}$ C in 96-well plates. Cells were pelleted by centrifugation and stained with phycoerythrin-conjugated anti-CD3 and allophycocyanin-conjugated anti-CD8 monoclonal antibodies prior to flow cytometric analysis. Analysis was performed with a FACSCalibur flow cytometer (BD Biosciences) using CellQuest software.

Peptides—Synthetic peptide preparations of hTERT-(865–873), hTERT-(540–548), and monosubstituted analogs were purchased from Pepsican Systems (Lelystad, The Netherlands). Human immunodeficiency virus-1 (HIV-1) Gag p17-(77–85) (SLYNTVATL) and human T cell lymphotropic virus-1 Tax-(11–19) (LLFGYPVYV) peptides were purchased from Invitrogen. The preparations used in this study were purified by mass spectrometry by the manufacturer and showed purities >95%. Powder was initially dissolved in Me₂SO and further diluted in serum-free RPMI 1640 medium to the desired concentrations.

Protein Synthesis—Soluble biotinylated monomeric pMHC I proteins were produced as described previously (34). Multimerization was performed by the addition of R-phycoerythrin-labeled streptavidin (Molecular Probes) to aliquots to a total pMHC I/streptavidin molar ratio of 4:1. Expression, refolding, purification, and biotinylation of soluble TCR heterodimers were conducted as described previously (35).

Surface Plasmon Resonance—A Biacore 3000 TM machine (Biacore, Uppsala, Sweden) and CM-5 sensor chips were used. Approximately 5000 response units of streptavidin were covalently linked to the chip surface in all four flow cells using the amino coupling kit according to the manufacturer's instructions. Biotinylated pMHC I proteins and biotinylated control

protein (HLA A2 PSCA1, HLA A2 MelanA, or HLA A2(D227K/T228A) MelanA) were bound to the sensor surfaces by flowing dilute solutions (50 $\mu\text{g}/\text{ml}$) of protein over the relevant streptavidin-coated flow cell. Approximately 1000 response units of protein ligand were bound to each flow cell for equilibrium affinity measurements. The soluble ILA1 TCR or CD8 $\alpha\alpha$ homodimer was then allowed to flow over the relevant flow cells at a rate of 5 $\mu\text{l}/\text{min}$ at the concentrations indicated in the figures. All measurements were performed at 25 $^{\circ}\text{C}$ using HEPES-buffered saline (0.01 M HEPES, pH 7.4, 0.15 M NaCl, 3 mM EDTA, and 0.005% Surfactant P20). Responses were recorded in real time and analyzed using BIAevaluation software (Biacore). Equilibrium dissociation constants (K_D) were determined assuming a 1:1 interaction ($A + B \rightleftharpoons AB$) by plotting specific equilibrium binding responses against protein concentrations, followed by nonlinear least-squares fitting of the Langmuir binding equation: $AB = AB_{\text{max}} \times B/(K_D + B)$. Conformation of the data to the Langmuir equation was confirmed by linear Scatchard plot analysis using Origin 6.0 software (MicroCal, Northampton, MA). The kinetics of TCR/pMHCI interactions were measured using sensor chips coated with 500 response units of ligand. Analyte TCR was flowed over the chip at a flow rate of 50 $\mu\text{l}/\text{min}$. First-order exponential association (k_a) and dissociation (k_d) curves were fitted simultaneously by nonlinear least squares.

pMHCI Tetramer Staining and Association and Dissociation Measurements—Staining of the various CTL lines and of the ILA1 CTL clone with tetramers was performed at a final concentration of 220 nM (with respect to the monomeric pMHCI component) unless stated otherwise. Titration staining experiments performed at 37 $^{\circ}\text{C}$ with cognate and non-cognate wild-type (WT) tetramers for clones ILA1 and 003 indicated that, with the tetramer preparations used in this study, non-cognate background staining remained negligible for concentrations ≤ 220 nM (data not shown). This concentration was thus chosen to perform standard CTL tetramer labeling. The staining conditions were 37 $^{\circ}\text{C}$ for 15 min or 4 $^{\circ}\text{C}$ for 45 min. For tetramer association, 10^6 ILA1 CTLs were washed and resuspended in 150 μl of phosphate-buffered saline; pMHCI tetramers were added at a final concentration of 1 $\mu\text{g}/\text{ml}$ (22 nM) with respect to monomer at t_0 . Aliquots of 10 μl of each sample were then taken at the indicated time points and diluted to a final volume of 500 μl in phosphate-buffered saline prior to flow cytometric analysis. Tetramer concentrations were thus diluted 50-fold so that further staining occurring after collection did not contribute significantly to the measured mean fluorescence intensity (MFI). Background staining obtained by labeling ILA1 CTLs with non-cognate HLA A2 tetramers for 30 min was subtracted from the MFI value at each time point. All stainings for the association kinetics were performed at room temperature. Detailed procedures for the tetramer decay assay are described elsewhere (36). Staining of ILA1 cells was performed with tetramer concentrations of 2.2 nM for 3G WT HLA A2 and HLA A2(D227K/T228A) tetramers, 8.8 nM for 8Y and 8T WT HLA A2 tetramers, and 220 nM for 8Y and 8T HLA A2(D227K/T228A) tetramers. Unless otherwise stated, CTL labeling was performed at 37 $^{\circ}\text{C}$ in azide buffer (phosphate-buffered saline, 0.1% NaN_3 , and 0.5% fetal calf serum). t_0 of the decay assay

refers to the addition of anti-HLA A2 monoclonal antibody (clone BB7.2, Serotec).

Tetramer Binding Kinetics and a Model for pMHCI Tetramer Staining—The model is based on the following assumptions. (i) A pMHCI tetramer approaching the cell surface from the incubation solution will initially engage a single TCR molecule. (ii) Subsequent TCR molecules are recruited to this “singlet” cluster by diffusing into the interaction radius of one of the tetramer binding sites and engaging that site, thus forming duplet and triplet clusters. (iii) Binding and rebinding to one of the three available tetramer binding sites occur very rapidly, so loss of temporarily unbound TCR molecules (by diffusion away from the tetramer domain of interaction) is negligible compared with loss by tetramer becoming unbound at all of its sites. (iv) Once a tetramer has become unbound, it will diffuse into solution, whereupon the TCR cluster is left with sufficient time to disband and diffuse into the background of free TCR molecules before the next tetramer binds one of these singlets from solution. (v) Within a triplet cluster, the transition from univalently bound tetramer to bivalently bound tetramer occurs at rate 6μ , where μ is the single-site TCR/pMHCI binding rate (three tetramer sites times two TCRs); the transition from bivalently bound tetramer to trivalently bound tetramer occurs at rate 2μ (as a single tetramer site remains available); the transition back from trivalently bound tetramer to bivalently bound tetramer occurs at rate 3ν (three bonds), where ν is the single-site dissociation rate; the transition from bivalently bound tetramer to univalently bound tetramer occurs at rate 2ν ; and the transition from univalently bound tetramer to unbound tetramer, which subsequently diffuses away into the solution while the TCR triplet dissolves, occurs at rate ν . The fraction of TCR triplets with n -valently bound tetramer ($n = 1, 2, 3$) is given by a quasi-stationary distribution that can be derived from the consideration of detailed balance equations based on the transition rates. For $n = 1$, this quasi-stationary value is approximately $(\nu/\mu)^2/2$, under the assumption that $\mu \gg \nu$. This means that triplet clusters disappear at a specific rate of $\nu(\nu/\mu)^2/2$. A similar argument can be developed for duplet clusters, giving the fraction $(\nu/\mu)2/3$ for univalently bound tetramers, which yields the formula $\nu(\nu/\mu)2/3$ for the corresponding specific duplet destruction rate. The univalent fraction for singlet clusters is 1, with destruction rate ν . Let R_n denote the density of clusters on the T cell surface where n denotes the status of the cluster ($n = 0, 1, 2, 3$; 0 is a “free” TCR molecule). Conservation of TCR molecules on the cell surface implies the following (Equation 1),

$$R_T = R_0 + R_1 + 2R_2 + 3R_3 \quad (\text{Eq. 1})$$

where R_T is the total density. The intensity of the stain (I) is assumed to be proportional to the sum $R_1 + R_2 + R_3$, which can be evaluated by calculating these values for a dynamic equilibrium between the various types of cluster. Singlet clusters form at rate ψR_0 , where ψ is the rate at which free TCR molecules capture a tetramer from solution. (This rate is proportional to the concentration of tetramer in the medium.) Singlet clusters break up at rate ν and recruit free TCR molecules at $\theta_1 R_0$. Duplet clusters break up at a rate of $\nu(\nu/\mu)2/3$ and recruit free

Coreceptor Dependence of CTL Activation and Tetramer Binding

TCR molecules at $\theta_2 R_0$. Triplet clusters break up at a rate of $\nu(\nu/\mu)^2/2$ and are incapable of recruiting additional TCR molecules. Setting creation and destruction rates equal for each of these species and assuming (i) that rates μ , ψ , θ_1 , and θ_2 are each proportional to the TCR/pMHC on-rate, whereas rate ν is proportional to the TCR/pMHC off-rate, and (ii) that the TCR recruitment rates are negligible in comparison with the break-up rates, we obtain two equations. First, the TCR conservation law becomes

$$1 = r_0 + (K_1/K_D)r_0 + 2(K_2/K_D)^3r_0^2 + 3(K_3/K_D)^6r_0^3 \quad (\text{Eq. 2})$$

where $r_0 = R_0/R_T$; K_D is the TCR/pMHC dissociation constant; and K_1 , K_2 , and K_3 are compound parameters absorbing the assumed proportionality relationships with the on-rates and off-rates. Given K_D , the conservation law can be solved for r_0 , and the relative intensity of the tetramer stain can then be calculated from Equation 3.

$$(R_1 + R_2 + R_3)/R_T = r_0 + (K_1/K_D)r_0 + (K_2/K_D)^3r_0^2 + (K_3/K_D)^6r_0^3 \quad (\text{Eq. 3})$$

Maximum staining intensity is attained when all TCR molecules are bound at a 1:1 stoichiometry to tetramers, *i.e.* when all TCR molecules are bound in singlets ($R_1 = R_T$). This does *not* correspond to the case in which K_D becomes vanishingly small; in that case, all TCR molecules are bound in triplets ($R_3 = R_T$), and the relative staining intensity is only one-third of the maximum. For data fitting, a standard least-squares procedure was employed, with minimization of the sum of squares by means of steepest descent. Equations 2 and 3 were solved by bisection. Data were log-transformed prior to the formation of the sum of squares, corresponding to a log-normal assumption on measurement noise and the standard procedure for homogenizing the variance. Estimates were expressed as the value that minimized the sum of squares \pm S.D., which is the square root of the estimated parameter variance, being the inverse second derivative of the sum of squares relative to the parameter, evaluated at the point estimate, times the error (noise variance) estimated by the sum of squares.

According to the kinetic assumptions listed above, the establishment of pMHC tetramer equilibrium staining is described by a complex nonlinear six-dimensional dynamic system. The staining intensity (I) is described by the following ordinary differential equation (Equation 4),

$$\dot{I} = \psi R_T - \lambda_{\text{eff}}(t)I \quad (\text{Eq. 4})$$

where $\lambda_{\text{eff}}(t)$ is a time-varying effective rate constant, which is a well defined function of the six-dimensional state of the system. Empirically, it is found that the association kinetics are an excellent fit to the biphasic exponential model

$$I(t) = I_{\text{max,fast}}(1 - \exp(-\lambda_{\text{fast}}t)) + I_{\text{max,slow}}(1 - \exp(-\lambda_{\text{slow}}t)) \quad (\text{Eq. 5})$$

(see Fig. 6, *A* and *B*). The parameters of this equation were determined by nonlinear least squares. It follows from Equa-

tion 5 that λ_{eff} relaxes to steady-state value $\lambda_{\text{eff}}(\infty)$, which can be calculated from the parameter estimates according to the formula $(I_{\text{max,fast}}\lambda_{\text{fast}} + I_{\text{max,slow}}\lambda_{\text{slow}})/(I_{\text{max,fast}} + I_{\text{max,slow}})$.

RESULTS

Diverse pMHC Binding Patterns Reflect Distinct Recognition Properties in Polyclonal and Monoclonal CTL Populations—Various CTL lines specific for HLA A2-restricted viral (HIV-1 Gag p17-(77–85) and human T cell lymphotropic virus-1 Tax-(11–19)) or tumor-derived (hTERT-(865–873)) peptides were established from antigen-experienced or antigen-naïve individuals and stained with cognate WT or CD8-null pMHC tetramers (Fig. 1, *A* and *B*); the latter were constructed from HLA A2 monomers containing a double D227K/T228A mutation in the $\alpha 3$ domain, which abrogates binding to the CD8 coreceptor (32). In CTL lines derived from antigen-experienced individuals, both WT and CD8-null pMHC tetramers identified cognate T cell populations of similar magnitude. However, the CD8-null tetramers consistently stained with lower MFI values compared with the WT tetramers at identical concentrations (Fig. 1, *A* and *B*). In contrast, a line specific for human T cell lymphotropic virus-1 Tax-(11–19) derived from an antigen-naïve individual (SH) stained only with the corresponding WT pMHC tetramer. Furthermore, antigen-responsive CTLs expanded from a naïve background by successive autologous stimulations with the hTERT-(865–873) peptide failed to bind either WT or CD8-null pMHC tetramers at any concentration (Fig. 1*A*) (data not shown), yet produced IFN- γ when exposed to cognate peptide (Fig. 1*C*). These data indicate that functional CTL populations can exhibit discrete tetramer binding profiles and CD8 dependences. Similar observations applied to different CTL clones (Fig. 1*D*) (data not shown). These distinct patterns of pMHC tetramer binding correlated with the efficiency of antigen recognition in IFN- γ release assays (Fig. 1*E*). Overall, these results indicate that CTLs with high levels of functional avidity can be selectively identified with CD8-null pMHC tetramers, as reported previously (37–39), whereas functional CTLs with low antigen sensitivity fail to bind WT or CD8-null pMHC tetramers.

Functional and Biophysical Characterization of hTERT-(540–548) Altered Peptide Ligands with Different Stimulatory Activities—Systematic screening of a library of monosubstituted peptide variants using the ILA1 CTL clone enabled us to identify an array of ligands that elicited distinct functional outcomes in cellular activation assays (data not shown). Two weak agonist, three superagonist, and an antagonist peptide were selected for further study (Fig. 2 and Table 1). The affinity of the ILA1 TCR for these various ligands was measured in surface plasmon resonance (SPR) binding equilibrium experiments. The measured dissociation constants spanned a wide spectrum of values (Fig. 3 and Table 1), from K_D values of 1 μM (close to the highest measured syngeneic interaction affinities) for 3G and 3G8T variants to high K_D values corresponding to very weak interactions (242 μM for 5Y). ILA1 TCR binding to the 8E weak agonist was so weak that we were unable to determine a reliable K_D from SPR binding equilibrium experiments (Fig. 3*H*). Interestingly, the non-stimulatory antagonist variant 7Y showed an affinity for the TCR substantially superior to the

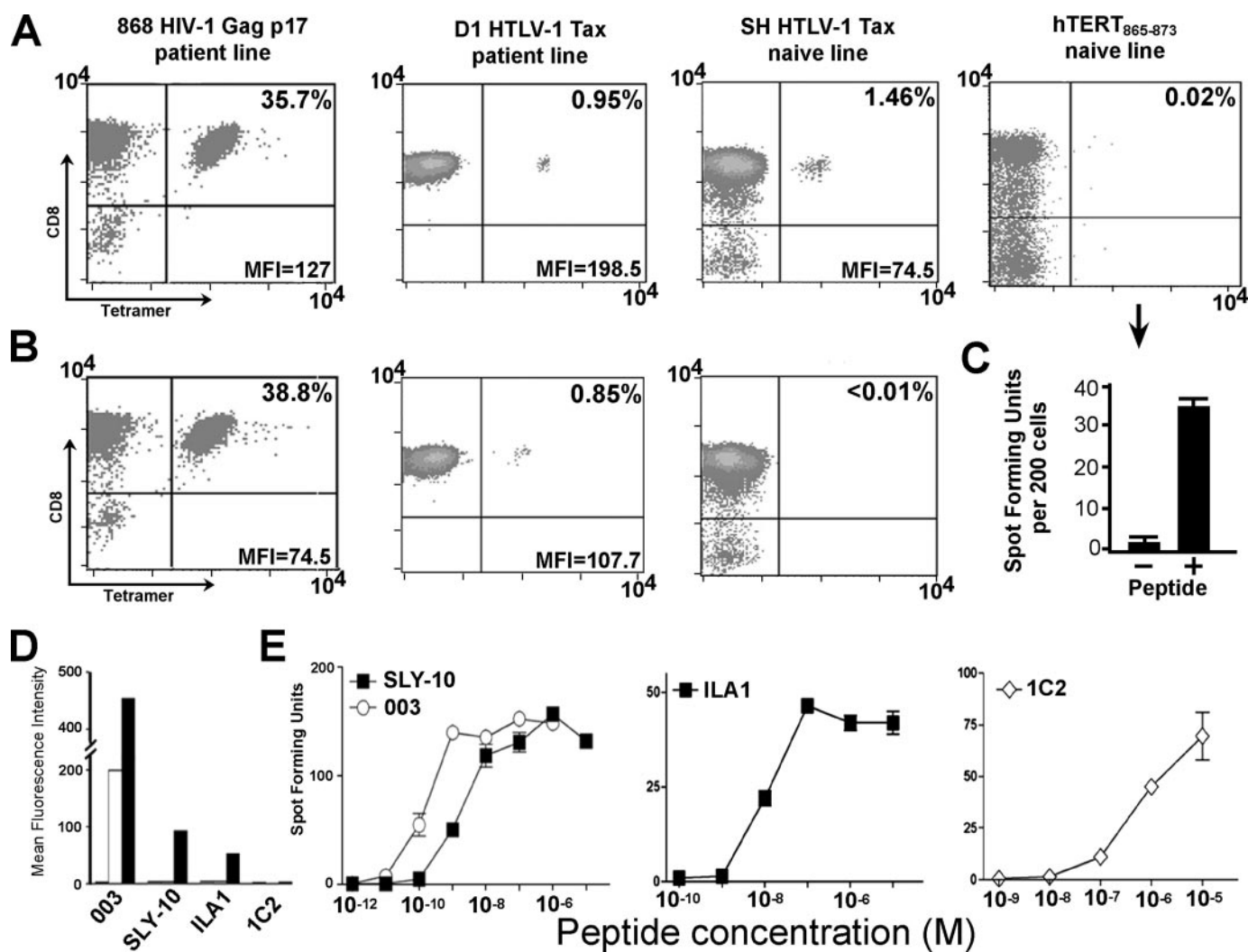


FIGURE 1. Heterogeneous pMHC tetramer staining patterns in various polyclonal and monoclonal CTL populations. A and B, HLA A2-restricted CTL lines from antigen-experienced or antigen-naïve donors, as indicated above each graph, were stained with cognate WT (A) or CD8-null (B) pMHC tetramers at a final concentration of 220 nM (10 μ g/ml). The frequency of tetramer-positive cells as a percentage of the total CD8⁺ population (upper right quadrant) and the FL-2 MFI of the CD8⁺/tetramer-positive population (lower right quadrant) are indicated in each case. C, in the case of the tetramer-negative CTL line specific for hTERT-(865–873), autologous presentation of cognate peptide resulted in antigen-specific activation in IFN- γ ELISpot assays; representative data are shown. D, the HLA A2-restricted CTL clones identified on the x axis were stained with cognate WT (black bars) and CD8-null (white bars) pMHC tetramers. Antigen specificities were as follows: 003 and SLY-10, HIV-1 Gag p17-(77–85); ILA1, hTERT-(540–548); and 1C2, hTERT-(865–873). The 1C2 clone was isolated by limiting dilution from the hTERT-(865–873) line depicted in A and C; experiments using 1C2 and antigen-presenting cells of different HLA haplotypes confirmed that hTERT-(865–873) presentation was HLA A2-restricted (data not shown). Clones 003 and SLY-10 were derived from HIV-infected donors; clone ILA1 was derived from an antigen-naïve individual. E, the peptide dose-response characteristics (“functional avidity”) of the clones shown in D were assessed in IFN- γ ELISpot activation assays with Hmy2.C1R cells transduced with WT HLA A2 as antigen-presenting cells as described under “Experimental Procedures.” The average number of spot-forming units and S.D. bars calculated from duplicates are shown.

weak agonist peptides 5Y and 8E (Fig. 3 and Table 1). There was an overall correlation between the potency of the various agonist ligands and their affinity for the ILA1 TCR, with the notable exception of the two high affinity superagonists 3G and 3G8T. Despite K_D values almost 10-fold lower than those measured for the two best superagonists (8Y and 8T), these two variants were less stimulatory in all cellular activation assays (Fig. 2 and Table 1) (data not shown). These results further serve to highlight that TCR/pMHC affinity is not the main correlate of ligand potency for cellular activation. Partial analysis of ILA1 agonist pMHC kinetic parameters was carried out to determine whether these ligands complied with the kinetic proofreading model of T cell activation and whether the high affinity for the ILA1 TCR of the relatively weak potency

ligands 3G and 3G8T could be explained by unusual kinetic features such as very fast on-rates. The association rate constant (k_{on}) for the 3G antigen was indeed substantially faster than those for the other ligands studied (Fig. 4 and Table 1). However, for the 3G altered peptide ligand, the dissociation rate constant (k_{off}) for the TCR/pMHC interaction was twice as slow compared with the most potent agonist, 8T (Table 1). Thus, the low potency of 3G compared with 8T could not be explained solely by the kinetic proofreading model. The kinetic parameters of the interaction between the ILA1 TCR and the weakest agonists 5Y and 8E were too fast for reliable measurement (Fig. 4). Nevertheless, it was apparent that the ILA1 TCR exhibited specific binding to both of these ligands. Comparison of the response unit traces

Coreceptor Dependence of CTL Activation and Tetramer Binding

for the 5Y and 8E ligands (Fig. 4, E and F) confirmed that 8E was a much poorer ligand than 5Y. Although it is not possible to give an accurate affinity for binding to the 8E variant from these experiments, it is clear that the K_D was $>500 \mu\text{M}$.

Tetramer Staining and TCR/pMHCI Interaction Affinity—The intensity or brightness of T cell labeling using pMHC tet-

ramers is generally thought to be an indicator of functional avidity and efficiency of antigen recognition in both MHCI (40, 41) and MHCII (42) systems. In the case of pMHCI tetramers, invariant binding of the CD8 coreceptor is also known to influence staining intensity. We used the ILA1 system to study the efficiency of pMHCI tetramer binding in relation to the affinity of the monomeric TCR/pMHCI interaction. At 37 °C, ILA1 CTLs stained at similar intensities with WT tetramers for which the monomeric pMHCI complex exceeded an affinity threshold for the TCR ($K_D < \sim 25 \mu\text{M}$); progressive decreases in tetramer binding were observed at higher K_D values (Fig. 5, A and C). Similar results were obtained with the corresponding CD8-null tetramers, although the drop-off set in at substantially higher affinities ($K_D < \sim 10 \mu\text{M}$) (Fig. 5, B and C). Staining was even more stringent when performed at 4 °C (Fig. 5D). In each case, the drop-off was sharp (occurring within about half a decade). This can be understood on the basis of tetramer binding kinetics. The monomeric K_D contributes to both the formation and persistence of a tetrameric bond to a TCR triplet cluster on the cell surface, yielding six multiplicative steps in the kinetics (see “Experimental Procedures” for details). Fitting a mathematical model to these kinetics indicated that the pMHCI/CD8 interaction prolongs the average monomeric TCR/pMHCI dwell time by a factor ~ 2.3 , in keeping with earlier estimates based on tetramer dissociation experiments (36).

Coreceptor Engagement and Soluble pMHCI Association and Dissociation Kinetics—A recent study documented that blocking the engagement between MHCI molecules and the CD8 coreceptor slows pMHCI tetramer association at the cell surface (22). As anti-CD8 antibodies seem to have a range of effects on pMHCI tetramer binding that do not reflect only disruption of the pMHCI/CD8 interaction (43, 44), we sought to reproduce this observation in the ILA1 system using CD8-null pMHCI tetramers. Three pMHCI ligands that showed significant staining in tetrameric form in the absence of CD8 binding (3G, 8T, and 8Y) (Fig. 5B) were selected for real-time binding analysis (Fig. 6, A and B). Data fitting showed a marked difference in the effective association rates between WT and CD8-

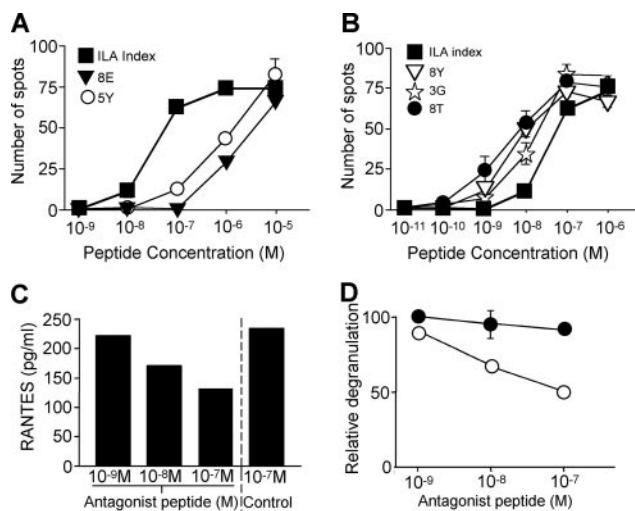


FIGURE 2. Functional characterization of hTERT-(540–548) peptide analogs with the ILA1 CTL clone. *A*, the peptide variants 5Y and 8E showed weak agonist properties as determined in IFN- γ ELISpot assays compared with the hTERT-(540–548) index peptide. *B*, three peptide variants (3G, 8T, and 8Y) showed improved stimulatory activity compared with the hTERT-(540–548) index peptide in IFN- γ ELISpot assays. *C*, immortalized B cells prepulsed with the 8T superagonist peptide (10^{-9} M) and incubated with the indicated concentrations of the 7Y antagonist or an irrelevant control peptide were used to stimulate ILA1 CTLs; RANTES (regulated on activation normal T cell expressed and secreted) release into the culture supernatant was measured by enzyme-linked immunosorbent assay (R&D Systems) according to the manufacturer’s instructions. *D*, shown is the antagonism of ILA1. CTL degranulation was measured by CD107a mobilization onto the cell surface; the assay was performed as described previously (33). Antigen-presenting cells were prepulsed with the 8T peptide (10^{-9} M) and incubated with the indicated concentrations of the 7Y peptide (○) for 6 h. Control experiments in which the irrelevant human T cell lymphotropic virus-1 Tax-(11–19) peptide (●) was added in place of the 7Y antagonist were conducted in parallel. Relative activity represents the ratio between the percentage of CD107a-positive CTLs activated by 8T peptide-pulsed B cells incubated with the indicated peptides and the percentage of CD107a-positive CTLs activated by 8T peptide-pulsed B cells only. In *A*, *B*, and *D*, assays were performed in duplicates; mean values and S.D. bars are shown. In *A* and *B*, ELISpot assays were performed using 250 cells/well.

TABLE 1

Recognition efficiency, binding equilibrium, and kinetic parameters of the epitope variants recognized by ILA1

EC_{50} values were determined from dose-response curves obtained by fitting the data of degranulation assays (see “Experimental Procedures”) to a nonlinear sigmoidal equation. The average EC_{50} value and S.D. for each ligand were calculated from three different experiments. NR, variants not recognized on CD8-null targets; ND, could not be reliably determined.

Parameter	Ligand				
	8E	5Y	Index	3G	8T
Log EC_{50} (M)					
WT HLA A2	$(3.55 \pm 1) \times 10^{-7}$	$(8.45 \pm 1) \times 10^{-8}$	$(2.7 \pm 0.5) \times 10^{-8}$	$(3.1 \pm 1.25) \times 10^{-9}$	$(9.7 \pm 2.33) \times 10^{-10}$
HLA A2(D227K/T228A)	NR	NR	$(6.7 \pm 0.66) \times 10^{-8}$	$(1.34 \pm 0.4) \times 10^{-8}$	$(3.4 \pm 0.15) \times 10^{-9}$
K_D (μM) ^a	>500	242 ± 20	36.6 ± 6.25	3.7 ± 0.28	27.6 ± 4.71
k_{on} ($\text{M}^{-1} \times \text{s}^{-1}$)	— ^b	— ^b	4.1×10^{-3}	1.6×10^{-4}	4×10^{-3}
k_{off} (s^{-1})	— ^b	— ^b	0.13	0.047	0.095
K_D (μM) ^c	ND	ND	32	2.9	23.75
Interaction $t_{1/2}$ (s) ^d			5.33	14.75	7.3

^a Determined from binding equilibrium experiments (see Fig. 3).

^b Too fast for reliable measurement.

^c Calculated from the kinetic parameters ($K_D = k_{off}/k_{on}$).

^d Calculated using the formula $t_{1/2} = \ln 2/k_{off}$.

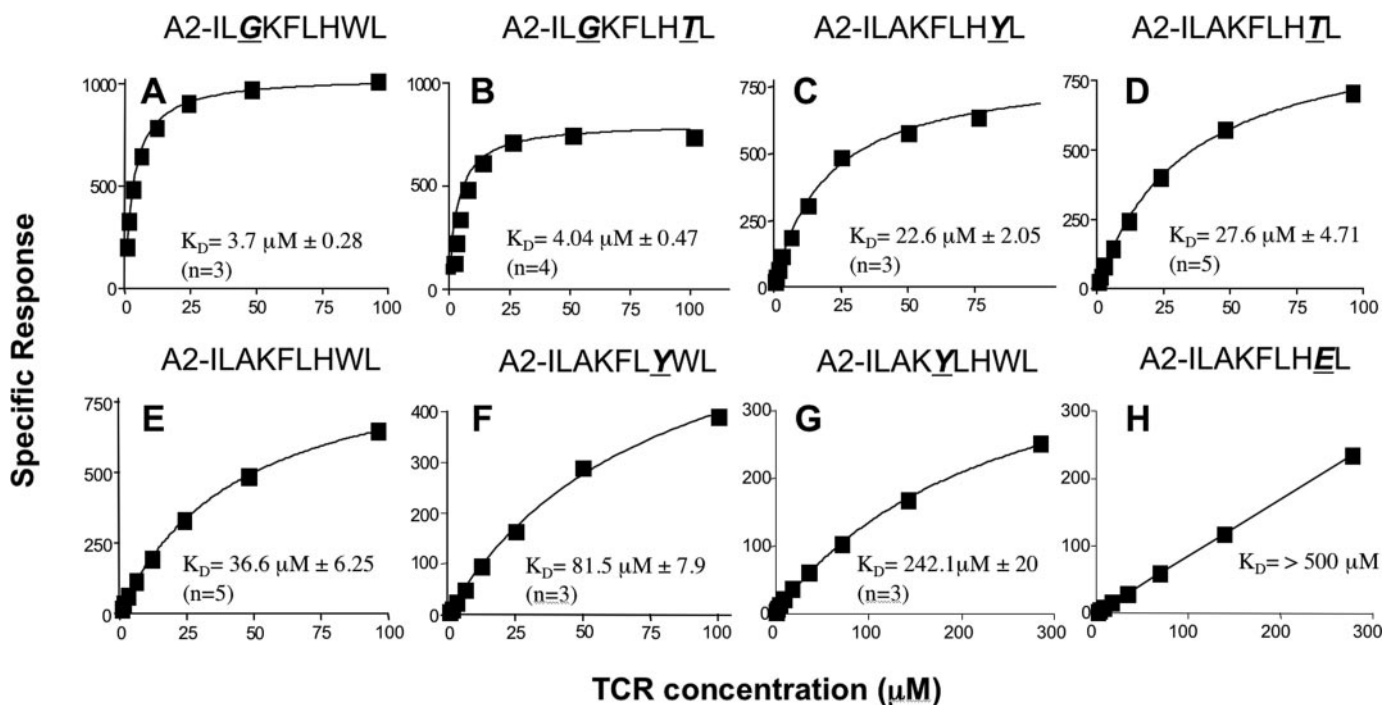


FIGURE 3. **Affinity measurements of the interaction between the ILA1 TCR and various cognate pMHC ligands.** The results from nonlinear analysis of SPR binding equilibrium experiments using soluble TCRs at a maximum concentration of 100 or 300 μM and 2-fold dilutions thereof flowed over immobilized pMHC complexes are shown here. K_D values were determined by analyzing the data in nonlinear curve fittings to the equation $AB = B \times AB_{\text{max}} / (K_D + B)$ assuming 1:1 Langmuir binding. Mean K_D values and the corresponding S.D. values are shown for each ligand. The integrity of pMHC proteins was verified by examining CD8 α binding using SPR (data not shown). Binding to the 8E variant was so weak that it failed to approach equilibrium even with the highest concentration of TCR utilized. Our estimates from both equilibrium binding and kinetic (Fig. 4) experiments with this ligand suggest a binding K_D of ~ 2 mM. However, these estimates are potentially subject to substantial errors. Comparison with experiments with the 5Y ligand (also see Fig. 4) confirmed that the ILA1 TCR interaction with the 8E variant ligand must be extremely weak ($K_D > 500$ μM).

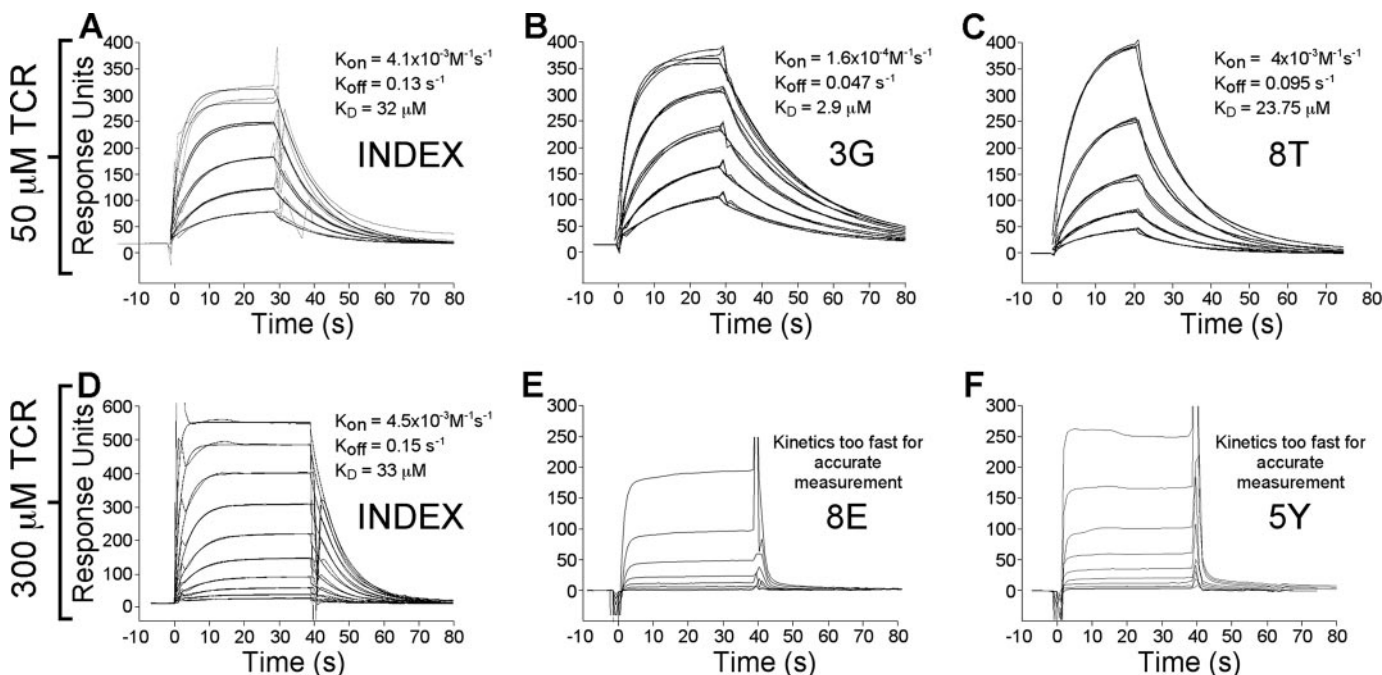


FIGURE 4. **Kinetic measurements of ILA1 TCR interactions with five different agonist pMHC ligands.** Upper panels, SPR kinetic measurements were performed with five serial 2-fold dilutions of 50 μM ILA1 TCR for the index (A), 3G (B), and 8T (C) variants. The plots show data and curve fitting from two separate experiments. Similar results ($\pm 5\%$) were obtained from three separate experiments with these protein preparations and from three other experiments using separately prepared pMHC and TCR preparations. Lower panels, 10 serial dilutions at a higher TCR concentration (300 μM) were used in an attempt to measure the binding with weak agonist ligands. Data obtained with the index ligand (D) were comparable with those obtained with the lower concentration (A) of separately prepared TCR and pMHC. However, the kinetics were too fast for accurate measurement for the 8E (E) and 5Y (F) ligands. All pMHC ligands bound equally well to the CD8 α protein (data not shown).

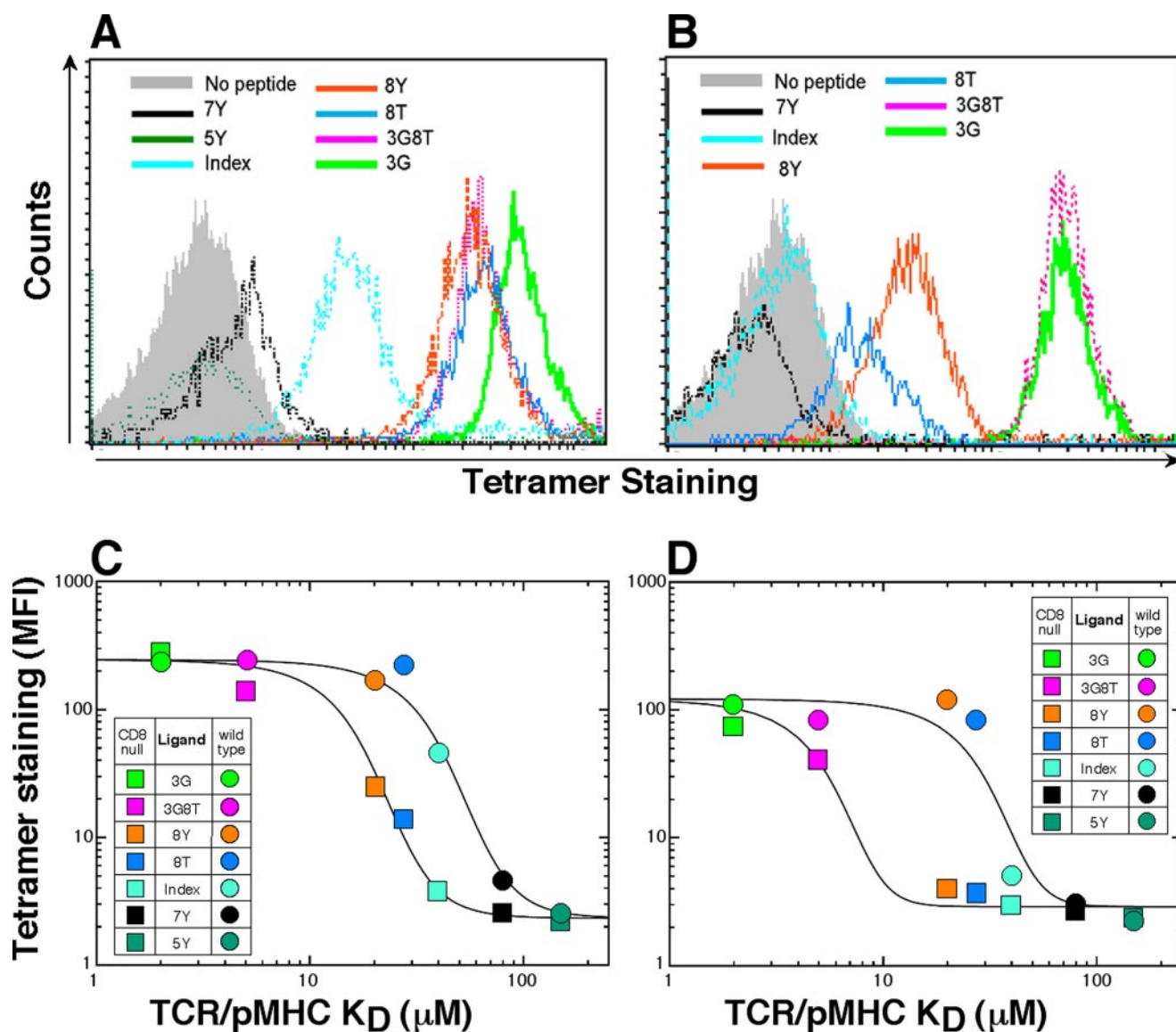


FIGURE 5. Staining of ILA1 CTLs with tetramerized cognate pMHC molecules. Shown is the staining of CTL clone ILA1 with seven different hTERT-(540–548) variants, as indicated, refolded with WT HLA A2 (A) or CD8-null HLA A2(D227K/T228A) (B) at 37 °C. The MFI values observed with pMHC tetramer staining are plotted versus the TCR/pMHC interaction K_D values for experiments conducted at 37 °C (C) and 4 °C (D) with WT HLA A2 (circles) and CD8-null HLA A2 (squares) molecules for each variant added at a final concentration of 220 nM (10 μ g/ml). Color codes correspond to those shown in A and B. Staining with the set of altered peptide ligands refolded with each type of heavy chain was performed at least three times. Representative data are shown. Curves are the best fit of the model described under “Experimental Procedures,” with estimates as follows: background staining, 2.32 ± 0.213 ; CD8 half-life prolongation factor (WT over CD8-null), 2.29 ± 0.08 ; $K_{2(WT)}$, $10.4 \pm 1.06 \mu$ M; $K_{3(WT)}$, $27.7 \pm 0.86 \mu$ M; K_1 fixed at 0 μ M; and maximum MFI signal fixed at 225.

null pMHC tetramers, consistent with observations by Gakamsky *et al.* (22). Calculation of $\lambda_{\text{eff}}(\infty)$ for tetramer staining kinetics (see “Experimental Procedures”) revealed that abrogation of the pMHC/CD8 interaction substantially reduced the capture rate of soluble pMHC tetramers by ILA1 CTLs. This reduction was estimated to be 61% for 3G, 85% for 8Y, and 90% for 8T.⁴ The stabilizing effect of the coreceptor was also assessed in the ILA1 system using pMHC tetramer decay assays (Fig. 6, C and D). In the case of 8T and 8Y altered peptide ligands, increasing the concentration of CD8-null tetramers did not result in staining intensity values similar to those obtained with WT tetramers used at 220 nM (data not shown); to achieve

similar MFI values for stainings with both types of tetramer, the concentrations of the WT HLA A2 tetramers were adjusted. As reported previously (36), abrogation of the pMHC/CD8 interaction markedly enhanced the tetrameric pMHC dissociation rate. All three selected pMHC complexes (3G, 8T, and 8Y) displayed similar dissociation patterns regardless of their respective affinities for the TCR. The interaction half-lives and dissociation kinetics for all three ligands in WT pMHC tetrameric form were nearly identical (Fig. 6C); the same held true for these ligands in CD8-null pMHC tetrameric form, although in each case, the $t_{1/2}$ values were approximately three times smaller. The increased avidity afforded by ligand multimerization thus seemed to have similar consequences on the stability of each complex regardless of the affinity of the corre-

⁴ H. A. van den Berg *et al.*, manuscript in preparation.

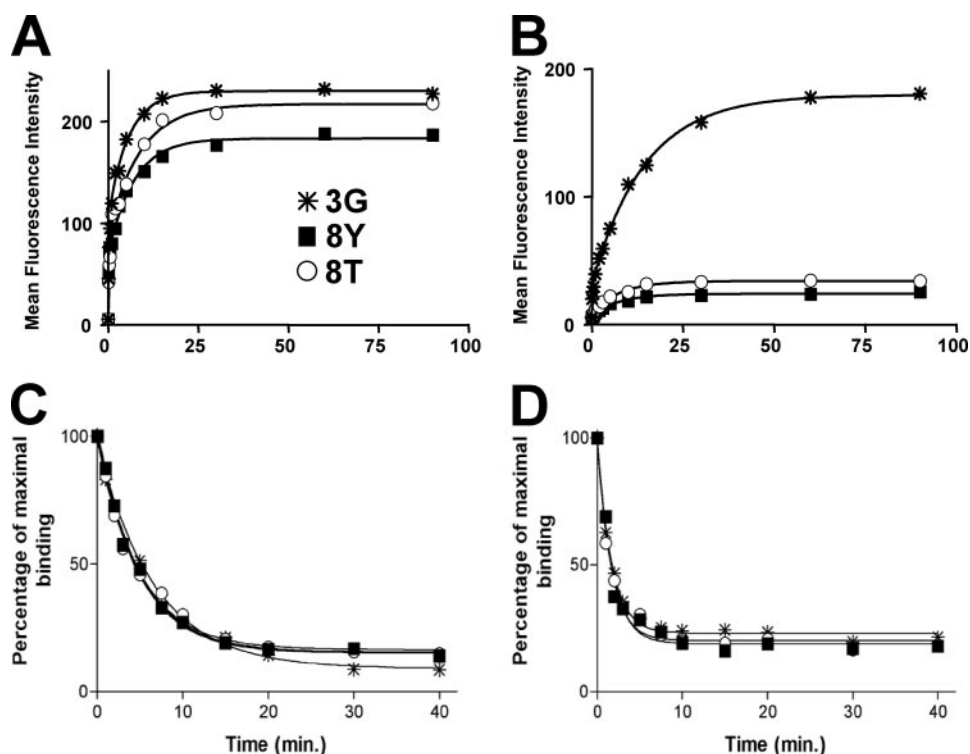


FIGURE 6. Real-time measurements of pMHC tetramer association and dissociation rates. Cell-surface association of various hTERT-(540–548) peptide variants refolded with WT HLA A2 (A) and HLA A2(D227K/T228A) (B) molecules was assessed by flow cytometry as described under “Experimental Procedures.” Data were fitted according to the biphasic exponential association equation (Equation 5). A, the association rate constants (λ_{fast}) of the fast phase derived from data analysis were 3.08 min^{-1} for 3G, 8.1 min^{-1} for 8T, and 3.07 min^{-1} for 8Y in the case of WT HLA A2. In the slow phase, the association rate constants (λ_{slow}) were 4.01 min^{-1} for 3G, 7.81 min^{-1} for 8T, and 4.45 min^{-1} for 8Y. B, in the context of HLA A2(D227K/T228A) tetramers, k_1 values were 0.18 min^{-1} for 3G, 0.14 min^{-1} for 8T, and 0.12 min^{-1} for 8Y; k_2 association constants were 0.07 min^{-1} for 3G, 0.13 min^{-1} for 8T, and 0.13 min^{-1} for 8Y. Estimation of time-varying effective rates (λ_{eff} ; see “Experimental Procedures”), reflecting the overall staining kinetics, were as follows. For WT HLA A2 tetramers, λ_{eff} values were 1.53 for 3G, 3.11 for 8T, and 1.3 for 8Y; for HLA A2(D227K/T228A) tetramers, λ_{eff} values were 0.76 for 3G, 2.34 for 8T, and 1.25 for 8Y. Consistent with the lower intensity staining observed in Fig. 5, the 8T and 8Y CD8-null tetramers exhibited substantially lower maximum staining levels in these association experiments. For the decay assays, azide-poisoned ILA1 CTLs were stained with pMHC tetramers at concentrations that resulted in equivalent fluorescence intensities (MFI = ~ 100) for each ligand in both WT (C) and CD8-null (D) forms. Data were fitted to the one-phase exponential decay equation: $y(t) = (y_{max} - y_{min}) \times (1 - \exp(-k_{off} \times t)) + y_{min}$. Interaction half-lives ($t_{1/2} = 0.69/k_D$) were 5.62 min for 3G, 3.37 min for 8T, and 3.42 min for 8Y in the context of WT HLA A2 molecules and 1.5 min for 3G, 1.18 min for 8T, and 1.14 min for 8Y in the context of CD8-null HLA A2 molecules. Stainings were carried out under identical conditions at least three times. Representative data are shown.

sponding monovalent interactions. Similarly, the coreceptor stabilizing effect monitored by the tetramer decay assays was nearly identical for all variants tested, as predicted previously (36).

Coreceptor Binding Is Strictly Required for the Engagement of Low Affinity Ligands by CTLs—The functional effects of pMHC/CD8 binding on cellular activation mediated by the ligands characterized in this study was assessed using Hmy2.C1R cells stably expressing either WT or CD8-null HLA A2 molecules (45). IFN- γ release and CD107a up-regulation on the cell surface were monitored (Fig. 7). In the context of the high affinity agonist ligands 8T and index, activation of ILA1 with antigen-presenting cells expressing either WT or CD8-null HLA A2 molecules showed a similar dynamic range of peptide concentrations (Fig. 7, A, B, E, and F). In contrast, abrogation of coreceptor binding inhibited activation by the low affinity peptide variants 5Y and 8E (Fig. 7, C, D, G, and H). Productive engagement of the lower affinity pMHC ligands by

the ILA1 TCR could be achieved only in the presence of coreceptor engagement even at high peptide densities. Thus, the degree of coreceptor dependence for CTL activation seems to be inversely correlated with the affinity and half-life of the TCR/pMHC interaction.

DISCUSSION

The experimental system described here enabled us to quantify the contribution made by CD8 invariant binding to cognate ligand engagement by CTLs under standardized conditions. Using soluble multimerized ligands, we have shown that CD8 substantially improves the binding efficiency of cognate pMHC molecules with intermediate to low affinities for the TCR. The observation that CD8 binding increases the number of stably bound pMHC complexes can be explained by enhancement of the association and/or reduction of the dissociation rates. The present data support a role for the coreceptor in both phenomena (Fig. 6). From a functional point of view and in light of the kinetic discrimination model of T cell activation, the increase in individual TCR/pMHC dwell times enabled by CD8 engagement would be expected to make a significant contribution to the well characterized enhancing effect that the coreceptor confers on the sensitivity of antigen recognition (36). In addition, as proposed by Pecht and Gakamsky (21), enhancement of the pMHC association rate by CD8 may also increase the overall number of productively engaged TCR complexes and thereby enhance the antigenicity of cognate ligands.

The magnitude of the coreceptor effect on the binding efficiency of cognate pMHC molecules was clearly influenced by monomeric TCR/pMHC affinities. At saturating concentrations of ligand, abrogation of CD8 engagement substantially reduced binding of tetrameric pMHC molecules exhibiting affinities for the TCR with K_D values in the range of 10 – $30 \mu\text{M}$ (Fig. 5). For TCR/pMHC interactions with $K_D \geq 30 \mu\text{M}$, coreceptor engagement became obligatory for tetramer binding. In contrast, functional assays with the same epitopes presented on the cell surface pointed to a lesser role for pMHC/CD8 extracellular binding in the process of CTL activation. In cellular activation experiments, dramatic inhibitory effects upon abrogation of pMHC/CD8 engagement were observed only in the case of the weakest agonists tested (5Y and 8E), even though all

Coreceptor Dependence of CTL Activation and Tetramer Binding

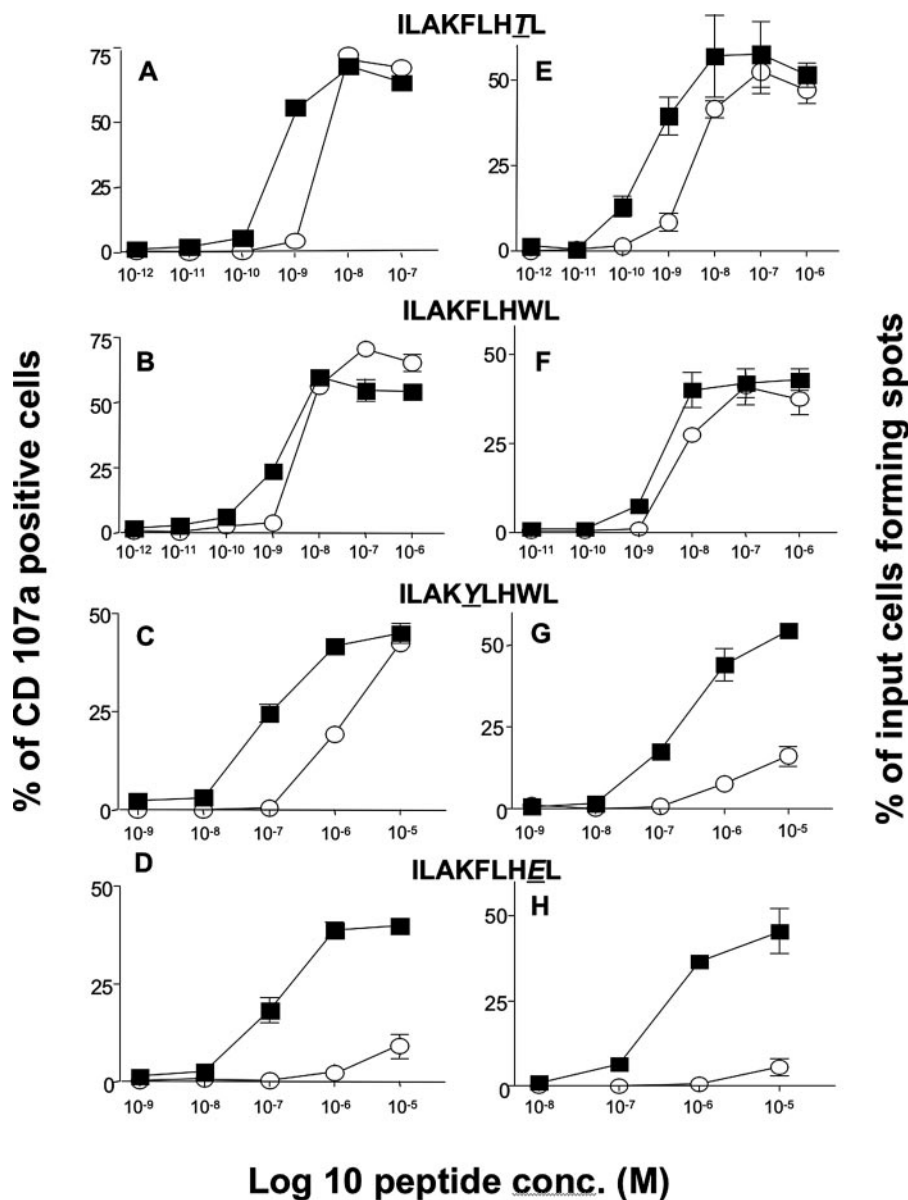


FIGURE 7. Effect of the CD8 coreceptor on antigenic recognition by ILA1 CTLs. *A–D*, the response of ILA1 to four different agonist ligands was determined in CD107a up-regulation assays. Each agonist peptide was presented by Hmy2.C1R cells expressing either CD8-null HLA A2(D227K/T228A) (○) or WT HLA A2 (■) molecules. Results are expressed as the percentage of effector cells showing significant activation. Means \pm S.D. were calculated from two sample replicates and are representative of at least two independent experiments in each case. *E–H*, IFN- γ secretion induced by peptide ligands presented in the context of WT (■) and CD8-null (○) HLA A2 molecules is expressed as a percentage of the total resting ILA1 CTLs added per sample. Error bars represent the S.D. of two replicate experiments.

of the different ligands tested showed a slight reduction in potency (Fig. 7 and Table 1). The 5Y variant displayed an affinity for the ILA1 TCR at the low end of previously characterized TCR/pMHC interactions with a K_D of 242 μM (Fig. 3). Both kinetic parameters and equilibrium binding analysis demonstrated that the ILA1 TCR bound to the 8E variant with an extremely low binding affinity ($K_D > 500 \mu\text{M}$). However, this ligand still elicited substantial activation in functional assays. Interestingly, the antigenicity of both the 5Y and 8E pMHC complexes was entirely dependent on intact MHC/coreceptor interactions. This suggests that enhancement of the TCR/pMHC association rate mediated by CD8 is crucial in deter-

mining the antigenicity of low affinity ligands with unusual kinetic features. Thus, although the degree of coreceptor dependence for tetramer binding and CTL activation is similarly dependent on monomeric TCR/pMHC affinity, there is a quantitative disparity between the binding effects of the coreceptor on soluble pMHC engagement and on activation by cell-surface determinants. Such a differential contribution of CD8 to tetramer binding and CTL activation had been suggested by the observation that CD8-negative cells bearing a TCR specific for an HLA A2-restricted hepatitis C virus epitope cannot bind tetramers, but are able to recognize this epitope displayed on the surface of antigen-presenting cells (46).

In apparent contradiction to kinetic proofreading models of T cell activation, the two ligands with the highest affinities for the TCR (Fig. 3) and the longest half-lives (3G and 3G8T) were not the most potent agonists (Figs. 2 and 4 and Table 1) (data not shown). Such inadequate behavior by T cell ligands has been described previously and has prompted researchers to develop and modify the kinetic proofreading concept. Notably, it lead to the integration of the notion of TCR-binding site plasticity, represented by the thermodynamic variable of heat change capacity, as an essential parameter governing T cell activation efficiency (47, 48). Alternatively, Yachi *et al.* (30) have recently proposed that exceptions to the kinetic proofreading dogma may result from impaired coreceptor recruitment to the vicinity of the TCR-CD3 complex because of unfav-

orable orientation of the TCR upon binding to pMHC. The data we report do not support this concept. First, detailed examination of 3G and 3G8T tetramer binding clearly indicated that CD8 contributes to the enhancement of both their association kinetics and the stability of bound complexes (Fig. 6) (data not shown), indicating that coreceptor engagement is not compromised in the case of these two ligands. Second, activation of ILA1 with antigen-presenting cells expressing HLA A2 molecules that cannot engage CD8 does not result in an inversion of the hierarchy of ligand potency between 3G and 8T, as would be predicted by the kinetic proofreading model (Fig. 7 and Table 1). Thus, our results argue in favor of a model

in which the CD8 dependence of cellular activation correlates with the relative affinities of the TCR for pMHC I complexes, as demonstrated by Holler and Kranz (27) in the 2C TCR system. However, the TCR/pMHC I affinity thresholds for CD8 dependence we observed in the human ILA1 system are very different from those proposed by these authors; their data showed that T cell activation is highly coreceptor-dependent for cognate TCR/pMHC I interactions with a K_D exceeding 3 μM . In our system, a high degree of coreceptor dependence was obvious only for low affinity interactions exhibiting K_D values in excess of 50 μM at the very least, even though abrogation of pMHC I/CD8 binding resulted in a marginal decrease in sensitivity for all high affinity ligands (Fig. 7 and Table 1). A fundamental difference in the experimental approach used in both studies might account for this discrepancy. Holler and Kranz used hybridomas transfected or not with CD8 α and CD8 β chains, whereas in our system, the pMHC I/coreceptor interaction was impaired by point mutations in the MHC I molecules. Normal levels of CD8 $\alpha\beta$ were expressed in the CTLs we used, and notably, there was no disruption to coreceptor association with the CD3 complex, the intracellular kinase Lck, or lipid rafts. Thus, our system dissociates the signaling functions and membrane partitioning roles of CD8, believed to be important in CTL activation, from its extracellular engagement of the MHC I molecules. Therefore, a likely explanation for the observed affinity threshold discrepancy is that increases in the association kinetics and stabilization of the TCR/pMHC I interaction afforded by CD8 extracellular binding are the sole phenomena accounting for the results we obtained in the ILA1 system. In contrast, disruption of the synergistic extracellular binding effects and intracellular coreceptor functions of CD8 in the system of Holler and Kranz probably resulted in a higher stringency of coreceptor dependence. A recent study suggested that the signaling properties of CD8 act in synergy with the TCR/pMHC I stabilization effect and are likely to have a dominant effect in the overall enhancement of the antigen sensitivity phenomenon conferred by the coreceptor (49). The difference of coreceptor dependence affinity thresholds observed in our study and in that of Holler and Kranz fits well with this concept. The fact that the murine pMHC I/CD8 interaction can be of >4 times higher affinity than the equivalent human interaction (32) is also likely to contribute to differences in the role of CD8 binding in the two species.

Overall, our data suggest that the dynamics of CD8 cell-surface expression, membrane segregation, and post-translational regulation known to modulate the state of responsiveness during T cell development alter the modalities of pMHC I binding, with important consequences for the engagement of lower affinity ligands in particular (Figs. 5 and 7). Notably, the differential contributions of pMHC I/CD8 interactions to the binding of soluble cognate ligands and CTL activation suggest that the intracellular coreceptor activities of CD8 exert their effect at least partially independently of extracellular pMHC I/CD8 engagement. Our findings also imply that rare polymorphisms in MHC I molecules that diminish CD8 binding, such as those that occur at posi-

tion 245 in HLA A68, HLA B48 and HLA B81, alter the influence of coreceptor engagement on CTL activation.

Our demonstration that CD8 substantially improves the binding efficiency of cognate pMHC I molecules with intermediate to low binding affinity for the TCR indicates that CD8 plays an important role in T cell cross-reactivity or "polyspecificity." It is well established that T cells are able to recognize a very large number of different peptides (reviewed in Ref. 50). Studies with murine hybridomas have shown that CD8 can alter the fine specificity of allogeneic (51) and syngeneic (27) recognition. Indeed, our own ongoing studies show that the majority of ligands recognized by CTL cannot be recognized at any peptide concentration in the absence of pMHC I/CD8 engagement. Thus, the CD8 coreceptor may serve to optimize T cell polyspecificity.

From a practical perspective, our data delineate the range of TCR/pMHC I affinities that are amenable to detection with fluorescent avidin-tetramerized pMHC I molecules. Ligands with K_D values <70–80 μM could be detected with WT pMHC I tetramers in our HLA A2-restricted system, whereas CD8-null pMHC I tetramers could label only ILA1 CTLs if the monovalent affinity for the TCR was higher ($K_D < 30 \mu\text{M}$) (Fig. 5). These results provide biophysical validation of the observations that CD8-null pMHC I tetramers can qualitatively distinguish CTL populations with high functional avidity (37–39) and confirm that staining intensity with tetramers correlates with functional avidity and TCR/pMHC I affinity (40, 41). It should be noted that parameters other than intrinsic affinity, such as variations of TCR density, differences in membrane lipid organization (52), the state of T cell activation (19, 53, 54), and differentiation status, can also influence tetramer binding avidity and are subject to substantial variation. These considerations preclude generalization of the tetramer staining affinity thresholds established in the system described here, in which all of these variables were standardized. Nevertheless, our results reveal the limitations of tetramer technology by providing direct evidence that functionally competent T cells can bear TCRs with affinities for cognate ligands below the threshold required for pMHC I tetramer engagement. Both human and murine "tetramer-negative" functional T cells have been reported previously (55–58). In one such system, Buslepp *et al.* (58) measured the affinity between the TCR and pMHC I by SPR; the K_D value of $\sim 80 \mu\text{M}$ they measured is consistent with our own results. Finally, our data suggest that soluble multimeric pMHC I molecules engineered to bind the coreceptor with enhanced affinities (36) might enable the detection of cognate ligands with extremely low affinities for the TCR, such as might characterize clonotypes specific for tumor-related or autologous antigens.

REFERENCES

1. Salter, R. D., Benjamin, R. J., Wesley, P. K., Buxton, S. E., Garrett, T. P., Clayberger, C., Krensky, A. M., Norment, A. M., Littman, D. R., and Parish, P. (1990) *Nature* **345**, 41–46
2. Konig, R., Huang, L. Y., and Germain, R. N. (1992) *Nature* **356**, 796–798
3. Cammarota, G., Scheirle, A., Takacs, B., Doran, D. M., Knorr, R., Banwarth, W., Guardiola, J., and Sinigaglia, F. (1992) *Nature* **356**, 799–801
4. Arcaro, A., Gregoire, C., Bakker, T. R., Baldi, L., Jordan, M., Goffin, L., Boucheron, N., Wurm, F., van der Merwe, P. A., Malissen, B., and Luescher, I. F. (2001) *J. Exp. Med.* **194**, 1485–1495

Coreceptor Dependence of CTL Activation and Tetramer Binding

- Rudd, C. E., Trevillyan, J. M., Dasgupta, J. D., Wong, L. L., and Schlossman, S. F. (1988) *Proc. Natl. Acad. Sci. U. S. A.* **85**, 5190–5194
- Veillette, A., Bookman, M. A., Horak, E. M., and Bolen, J. B. (1988) *Cell* **55**, 301–308
- Zamoyska, R. (1998) *Curr. Opin. Immunol.* **10**, 82–87
- Miceli, M. C., and Parnes, J. R. (1993) *Adv. Immunol.* **53**, 59–122
- Norment, A. M., and Littman, D. R. (1988) *EMBO J.* **7**, 3433–3439
- Gangadharan, D., and Cheroutre, H. (2004) *Curr. Opin. Immunol.* **16**, 264–270
- Gao, G. F., Tormo, J., Gerth, U. C., Wyer, J. R., McMichael, A. J., Stuart, D. I., Bell, J. I., Jones, E. Y., and Jakobsen, B. K. (1997) *Nature* **387**, 630–634
- Norment, A. M., Salter, R. D., Parham, P., Engelhard, V. H., and Littman, D. R. (1988) *Nature* **336**, 79–81
- Chang, H. C., Tan, K., Ouyang, J., Parisini, E., Liu, J. H., Le, Y., Wang, X., Reinherz, E. L., and Wang, J. H. (2005) *Immunity* **23**, 661–671
- Leishman, A. J., Naidenko, O. V., Attinger, A., Koning, F., Lena, C. J., Xiong, Y., Chang, H. C., Reinherz, E., Kronenberg, M., and Cheroutre, H. (2001) *Science* **294**, 1936–1939
- Daniels, M. A., Devine, L., Miller, J. D., Moser, J. M., Lukacher, A. E., Altman, J. D., Kavathas, P., Hogquist, K. A., and Jameson, S. C. (2001) *Immunity* **15**, 1051–1061
- Moody, A. M., Chui, D., Reche, P. A., Priatel, J. J., Marth, J. D., and Reinherz, E. L. (2001) *Cell* **107**, 501–512
- Couedel, C., Bodinier, M., Peyrat, M. A., Bonneville, M., Davodeau, F., and Lang, F. (1999) *J. Immunol.* **162**, 6351–6358
- Demotte, N., Colau, D., Ottaviani, S., Godelaine, D., Van Pel, A., Boon, T., and van der Bruggen, P. (2002) *Eur. J. Immunol.* **32**, 1688–1697
- Kao, C., Daniels, M. A., and Jameson, S. C. (2005) *Int. Immunol.* **12**, 1607–1617
- Maile, R., Siler, C. A., Kerry, S. E., Midkiff, K. E., Collins, E. J., and Frelinger, J. A. (2005) *J. Immunol.* **174**, 619–627
- Pecht, I., and Gakamsky, D. M. (2005) *FEBS Lett.* **579**, 3336–3341
- Gakamsky, D. M., Luescher, I. F., Pramanik, A., Kopito, R. B., Lemonnier, F., Vogel, H., Rigler, R., and Pecht, I. (2005) *Biophys. J.* **89**, 2121–2133
- al-Ramadi, B. K., Jelonek, M. T., Boyd, L. F., Margulies, D. H., and Bothwell, A. L. (1995) *J. Immunol.* **155**, 662–673
- Cho, B. K., Lian, K. C., Lee, P., Brunmark, A., McKinley, C., Chen, J., Kranz, D. M., and Eisen, H. N. (2001) *Proc. Natl. Acad. Sci. U. S. A.* **98**, 1723–1727
- Guimezanes, A., Montero-Julian, F., and Schmitt-Verhulst, A. M. (2003) *Eur. J. Immunol.* **33**, 3060–3069
- Viola, A., Salio, M., Tuosto, L., Linkert, S., Acuto, O., and Lanzavecchia, A. (1997) *J. Exp. Med.* **186**, 1775–1779
- Holler, P. D., and Kranz, D. M. (2003) *Immunity* **18**, 255–264
- Kerry, S. E., Buslepp, J., Cramer, L. A., Maile, R., Hensley, L. L., Nielsen, A. I., Kavathas, P., Vilen, B. J., Collins, E. J., and Frelinger, J. A. (2003) *J. Immunol.* **171**, 4493–4503
- Buslepp, J., Wang, H., Biddison, W. E., Appella, E., and Collins, E. J. (2003) *Immunity* **19**, 595–606
- Yachi, P. P., Ampudia, J., Zal, T., and Gascoigne, N. R. (2006) *Immunity* **25**, 203–211
- Laugel, B., Boulter, J. M., Lissin, N., Vuidepot, A., Li, Y., Gostick, E., Crotty, L. E., Douek, D. C., Hemelaar, J., Price, D. A., Jakobsen, B. K., and Sewell, A. K. (2005) *J. Biol. Chem.* **280**, 1882–1892
- Purbhoo, M. A., Boulter, J. M., Price, D. A., Vuidepot, A. L., Hourigan, C. S., Dunbar, P. R., Olson, K., Dawson, S. J., Phillips, R. E., Jakobsen, B. K., Bell, J. I., and Sewell, A. K. (2001) *J. Biol. Chem.* **276**, 32786–32792
- Betts, M. R., Brenchley, J. M., Price, D. A., De Rosa, S. C., Douek, D. C., Roederer, M., and Koup, R. A. (2003) *J. Immunol. Methods* **281**, 65–78
- Glick, M., Price, D. A., Vuidepot, A. L., Andersen, T. B., Hutchinson, S. L., Laugel, B., Sewell, A. K., Boulter, J. M., Dunbar, P. R., Cerundolo, V., Oxenius, A., Bell, J. I., Richards, W. G., and Jakobsen, B. K. (2002) *J. Biol. Chem.* **277**, 20840–20846
- Boulter, J. M., Glick, M., Todorov, P. T., Baston, E., Sami, M., Rizkallah, P., and Jakobsen, B. K. (2003) *Protein Eng.* **16**, 707–711
- Wooldridge, L., van den Berg, H. A., Glick, M., Gostick, E., Laugel, B., Hutchinson, S. L., Milicic, A., Brenchley, J. M., Douek, D. C., Price, D. A., and Sewell, A. K. (2005) *J. Biol. Chem.* **280**, 27491–27501
- Choi, E. M., Chen, J. L., Wooldridge, L., Salio, M., Lissina, A., Lissin, N., Hermans, I. F., Silk, J. D., Mirza, F., Palmowski, M. J., Dunbar, P. R., Jakobsen, B. K., Sewell, A. K., and Cerundolo, V. (2003) *J. Immunol.* **171**, 5116–5123
- Pittet, M. J., Rubio-Godoy, V., Bioley, G., Guillaume, P., Batard, P., Speiser, D., Luescher, I., Cerottini, J. C., Romero, P., and Zippelius, A. (2003) *J. Immunol.* **171**, 1844–1849
- Price, D. A., Brenchley, J. M., Ruff, L. E., Betts, M. R., Hill, B. J., Roederer, M., Koup, R. A., Migueles, S. A., Gostick, E., Wooldridge, L., Sewell, A. K., Connors, M., and Douek, D. C. (2005) *J. Exp. Med.* **202**, 1349–1361
- Yee, C., Savage, P. A., Lee, P. P., Davis, M. M., and Greenberg, P. D. (1999) *J. Immunol.* **162**, 2227–2234
- Busch, D. H., and Pamer, E. G. (1999) *J. Exp. Med.* **189**, 701–710
- Crawford, F., Kozono, H., White, J., Marrack, P., and Kappler, J. (1998) *Immunity* **8**, 675–682
- Wooldridge, L., Scriba, T. J., Milicic, A., Laugel, B., Gostick, E., Price, D. A., Phillips, R. E., and Sewell, A. K. (2006) *Eur. J. Immunol.* **36**, 1847–1855
- Wooldridge, L., Hutchinson, S. L., Choi, E. M., Lissina, A., Jones, E., Mirza, F., Dunbar, P. R., Price, D. A., Cerundolo, V., and Sewell, A. K. (2003) *J. Immunol.* **171**, 6650–6660
- Hutchinson, S. L., Wooldridge, L., Tafuro, S., Laugel, B., Glick, M., Boulter, J. M., Jakobsen, B. K., Price, D. A., and Sewell, A. K. (2003) *J. Biol. Chem.* **278**, 24285–24293
- Callender, G. G., Rosen, H. R., Roszkowski, J. J., Lyons, G. E., Li, M., Moore, T., Brasic, N., McKee, M. D., and Nishimura, M. I. (2006) *Hepatology* **43**, 973–981
- Garcia, K. C., Radu, C. G., Ho, J., Ober, R. J., and Ward, E. S. (2001) *Proc. Natl. Acad. Sci. U. S. A.* **98**, 6818–6823
- Krogsgaard, M., Prado, N., Adams, E. J., He, X. L., Chow, D. C., Wilson, D. B., Garcia, K. C., and Davis, M. M. (2003) *Mol. Cell* **12**, 1367–1378
- Lyons, G. E., Moore, T., Brasic, N., Li, M., Roszkowski, J. J., and Nishimura, M. I. (2006) *Cancer Res.* **66**, 11455–11461
- Mason, D. (1998) *Immunol. Today* **19**, 395–404
- Blok, R., Margulies, D. H., Pease, L., Ribaud, R. K., Schneck, J., and McCluskey, J. (1992) *Int. Immunol.* **4**, 455–466
- Drake, D. R., III, and Braciale, T. J. (2001) *J. Immunol.* **166**, 7009–7013
- Fahmy, T. M., Bieler, J. G., Edidin, M., and Schneck, J. P. (2001) *Immunity* **14**, 135–143
- Drake, D. R., III, Ream, R. M., Lawrence, C. W., and Braciale, T. J. (2005) *J. Immunol.* **175**, 1507–1515
- Burrows, S. R., Kienzle, N., Winterhalter, A., Bharadwaj, M., Altman, J. D., and Brooks, A. (2000) *J. Immunol.* **165**, 6229–6234
- Falta, M. T., Fontenot, A. P., Rosloniec, E. F., Crawford, F., Roark, C. L., Bill, J., Marrack, P., Kappler, J., and Kotzin, B. L. (2005) *Arthritis Rheum.* **52**, 1885–1896
- Hernandez, J., Lee, P. P., Davis, M. M., and Sherman, L. A. (2000) *J. Immunol.* **164**, 596–602
- Buslepp, J., Kerry, S. E., Loftus, D., Frelinger, J. A., Appella, E., and Collins, E. J. (2003) *J. Immunol.* **170**, 373–383